JOURNAL OF COMPUTATIONAL PHYSICS 105, 339–353 (1993)

A Numerical Implementation of MHD in Divergence Form*

MAURICE H. P. M. VAN PUTTEN†

Theoretical Astrophysics 130-33 and Applied Mathematics 217-50, Caltech, Pasadena, California 91125

Received November 6, 1991

A numerical implementation of fully relativistic MHD in divergence form for the purpose of shock computations is presented. We illustrate the implementation on the coplanar Riemann problem for MHD. The computations are performed using a pseudo-spectral method. Brio and Wu recently demonstrated the existence of compound waves in classical MHD. We find that compound waves persist in relativistic MHD. Two limiting cases are considered numerically: a limit in which the velocities become nonrelativistic, and a limit in which the longitudinal magnetic field approaches zero. A comparison is made with the results of nonrelativistic MHD, and with the singular case of zero longitudinal magnetic field.

1. INTRODUCTION

Numerical simulation of hydrodynamics and magnetohydrodynamics has become increasingly important in the field of astrophysics. Interpretation of the structure, origin, and long time evolution of astrophysical flow is approached today succesfully by large scale numerical simulations using nonrelativistic codes [18]. Much of these numerical studies is on the morphology of jets, which show intricate patterns of shocks. Radio-astronomy has provided us with detailed images of these flows on the kiloparsec scale. Lind [12] emphasizes that these simulations are to be regarded as qualitative investigations. In particular, he expresses caution in the interpretation of numerical simulations of jets on the parsec scale, where they are believed to be highly relativistic. Extension of numerical simulations to relativistic hydrodynamics has received much attention by many authors (see, e.g., [15, 16, 18, 13]). Furthermore, magnetic fields are believed to be present in these flows. Magnetic fields are important in radiative phenomena (Phinney [8]) and in the structure of astrophysical flow [8, 18]. Numerical simulation of relativistic MHD has been considered most notably by Evans and Hawley [22] and, recently, by Dubal [19].

In [25] we presented a divergence formulation of locally adiabatic relativistic MHD for the purpose of numerical simulation. We showed that MHD in divergence form allows for numerical simulation of the problem of wave breaking in one dimension up to the moment of breaking. The purpose of this paper is to demonstrate that MHD in divergence form also allows for numerical simulation of more complicated MHD flow with shocks. To this end we seek

(a) *MHD in divergence form whose standard jump* conditions across surfaces of discontinuity are the physical, enthalpy preserving jump conditions across shocks;

(b) A *numerical method for MHD in divergence form* for the purpose of shock computations;

(c) A one-dimensional shock-tube problem which features many of the possible MHD shocks.

The first item will be obtained by a rewriting of the result from [25]. The resulting system is equivalent to the former whenever the flow is continuously differentiable.

Several illustrative examples will be computed. Using a pseudo-spectral method with explicit time-stepping on a uniform grid we further show the effectiveness of the divergence formulation of MHD. Brio and Wu [17] computed the coplanar Riemann problem in classical, nonrelativistic MHD. In this paper, we will study the same problem for relativistic MHD. A pseudo-spectral method is employed which is tested against an analytical solution in a Riemann shock-tube problem in the singular limit of a purely transverse magnetic field. In [17] Brio and Wu showed the existence of a compound wave (a shock wave with attached to it a rarefaction wave of the same family) in nonrelativistic MHD. These results have recently also been computed by Stone *et al.* [24]. We will find that compound waves persist in relativistic MHD as a natural continuation of Brio and Wu's nonrelativistic result.

MHD in divergence form is a constraint-free formulation

* This work has been supported by NASA Grant NAGW-2394.

† Present address: Institute for Theoretical Physics, University of Santa Barbara, CA 93016.

0021-9991/93 $5.00

based on taking constraints as conserved quantities [25]. We remark that this method of treating constraints may have applications to other systems of equations. The results in this paper can be taken as demonstration of this method *an sich* in the particular context of MHD.

In Section 2, MHD is formulated in divergence form which allows for the computation of shocks. Our pseudo-spectral method is outlined in Section 3, together with a test on the Riemann shock-tube problem with transverse magnetic field. The relativistic generalization of Brio and Wu's coplanar Riemann problem is presented in Section 4. Two limits are considered numerically: a limit in which the velocities become nonrelativistic, and a limit in which the longitudinal magnetic field approaches zero. Particular attention is given to see that our numerical implementation of relativistic MHD retains nonrelativistic MHD in the limit of low velocities, low pressures, and low magnetic field energies.

2. FORMULATION OF THE PROBLEM

The problem of numerical simulation of relativistic MHD flow in the presence of shocks is considered by formulating the equations of MHD in divergence form. This approach has been motivated by the computational methods used in nonrelativistic computational fluid dynamics. In divergence form the equations of MHD are amenable to numerical implementation by shock capturing schemes, provided that the jump conditions that follow from a weak formulation are the physical jump conditions of conservation of energy and momentum, baryon number, and those of Maxwell's equations. The theory of MHD in covariant form has been discussed by many authors (see, e.g., [26, 3, 1]) and the equations are briefly introduced here.

The fluid is considered to be perfect in that viscosity and thermal conductivity are neglected. A perfectly conducting fluid with velocity four-vector u^a in the presence of an electromagnetic field with magnetic field four-vector, h^a, is described by a stress-energy tensor of the form

$$T^{ab} = \rho u^a u^b + P^* g^{ab} - h^a h^b, \tag{1}$$

where $\rho = rf + h^2$ and $P^* = P + h^2/2$ with r the proper rest mass density, f the specific enthalpy, and P the hydrostatic pressure. The quantities r, P, and f are related to the entropy, S, and the temperature, T, by $dP = r\,df + rT\,dS$. The specific enthalpy f takes the form $f = 1 + (\gamma/(\gamma-1))P/r$ for a fluid with polytropic equation of state, $P = Kr^\gamma$, and polytropic index, γ. In regions where the fluid variables are continuously differentiably, these quantities satisfy the conservation of energy and momentum, Maxwell's equations, conservation of baryon number, and local adiabaticity (ideal MHD),

$$\begin{aligned} \nabla_a T^{ab} &= 0, \\ \nabla_a (u^{[a} h^{b]}) &= 0, \\ c(U) := u^c h_c &= 0, \\ \nabla_a (r u^a) &= 0, \\ u^a \nabla_a S &= 0, \end{aligned} \tag{2}$$

respectively. Here, $c(U) = 0$ constitutes a constraint equation. With $c(U) = 0$ the vector field h_a represents the magnetic field in the rest frame of the fluid, and (2) uniquely defines the evolution of the variables $U = (u^a, h^a, r, P)$. In view of constraint equation $c(U) = 0$, (2) forms a partial differential-algebraic system equations, whose numerical implementation is difficult in particular in the presence of shocks. Evidently, the constraint $c(U) = 0$ is to be satisfied in numerical simulations for a solution to be an MHD solution.

The equations of ideal MHD, including the flux-freezing constraint (2) can be written in constraint-free divergence form as [25]

$$\begin{aligned} \nabla_a T^{ab} &= 0, \\ \nabla_a \{ (u^{[a} h^{b]} + g^{ab} c(U) \} &= 0, \\ \nabla_a (r u^a) &= 0, \\ \nabla_a (r S u^a) &= 0. \end{aligned} \tag{3}$$

In the case of (3) the jump conditions across surfaces of discontinuity that follow from a weak formulation (see, e.g., [6]) yield strict adiabaticity, because of the last two equations. For this reason, we rewrite this system (3) such that these standard jump conditions associated with it contain the entropy increasing jump conditions across shocks. In regions where the flow is smooth, we have

THEOREM 2.1. *The equations of locally adiabatic ideal MHD including the flux-freezing constraint can be stated as*

$$\nabla_a F^{aA} \equiv \begin{cases} \nabla_a T^{ab} = 0, \\ \nabla_a \{ u^{[a} h^{b]} + g^{ab} c(U) \} = 0, \\ \nabla_a (r u^a) = 0, \\ \nabla_a \{ (u^c u_c + 1)\, \xi^a \} = 0, \end{cases} \tag{4}$$

where ξ^a is any prescribed time-like vector field. This system is equivalent to (3) *in regions where the flow is continuously differentiable. The standard jump conditions across surfaces of discontinuity for this system are those of conservation of energy-momentum, baryon number, and Maxwell's equations.*

Note that Maxwell's equations imply the identity

$$u_b \nabla_a T^{ab} \equiv u_b \nabla^a (rfu^a u^b + Pg^{ab}). \tag{5}$$

Consequently, the equation of continuity and the thermodynamic relation $dP = r\,df - rT\,dS$ yield

$$u_b \nabla_a T^{ab} \equiv f(ru^a)\nabla_a u^2/2 + (u^2+1)(u^a\nabla_a)P + Tu^2(ru^a)\nabla_a S. \tag{6}$$

It follows that conservation of either one of the relations

$$\begin{aligned} u^2 + 1 &= 0, \\ u^a \nabla_a S &= 0 \end{aligned} \tag{7}$$

implies the other. Thus, for smooth flow the two systems (3) and (4) are equivalent. Furthermore, the jump conditions across a surface of discontinuity with normal one-form, v_a, as follows from a weak formulation of (4) are

$$\begin{aligned} [T^{ab}]\, v_a &= 0, \\ [u^{[a}h^{b]} + g^{ab}c(U)]\, v_a &= 0, \\ [ru^a]\, v_a &= 0, \\ [(u^c u_c + 1)]\, \xi^a v_a &= 0. \end{aligned} \tag{8}$$

Here, $[q] = (q)^+ - (q)^-$ denotes the jump in q across the shock. Evidently, jump conditions (8) contain conservation of energy-momentum and baryon number. It is shown in [25, Proposition 3.1], that $c(U) := u^c h_c = 0$ is preserved across shocks. Finally, the last equation in (8) ensures that also the condition $u^c u_c + 1 = 0$ is preserved, provided that ξ^a is not tangential to the shock surface, $\xi^a v_a \neq 0$. This establishes the theorem.

We remark that $\xi^a \equiv$ const. yields a quadratically nonlinear system in the hydrodynamical limit to which Roe's linearization (see [21]) can be applied in a straightforward manner. When $h^a \equiv 0$, we obtain

$$\begin{aligned} \nabla_a (w^a w^b + sp) &= 0, \\ \nabla_a \left\{ \left(s - \frac{\gamma}{\gamma - 1} p \right) w^a \right\} &= 0, \\ \nabla_a \{ (w^c w_c + s^2)\, \xi^a \} &= 0, \end{aligned} \tag{9}$$

with characteristic determinant (cf. Proposition 5.1 in [25]),

$$D = (\xi^a v_a)(w^a v_a)(a_1 (w^a v_a)^2 - a_2 (v^a v_a)), \tag{10}$$

where $a_1 = (2/(\gamma-1))(\gamma p - s)$ and $a_2 = ((\gamma/(\gamma-1))\, p + s)\, w^c w_c + (s - (\gamma/(\gamma-1))\, p)\, s^2$. Here, $w^a = \sqrt{rf}\, u^a$, $s = \sqrt{rf}$, $p = P/\sqrt{rf}$, and v_a is a one-form. Thus, Roe's linearization yields a linear Riemann solver in terms of six null vectors which we have found can readily be implemented. However, a Roe solver for MHD is expected to be rather complex and, by similar arguments, possible in analytic form only when $\gamma = 2$ as in [17]. Therefore, we will not elaborate on this further here.

A pseudo-spectral method is used for all our computations. This method is first applied in a Riemann shock-tube problem with purely transverse magnetic field for a fluid with $\gamma = \frac{3}{2}$ in view of an analytical solution in this case. We will also apply this method to Bri and Wu's coplanar Riemann problem in classical MHD.

3. DESCRIPTION OF THE METHOD

In astrophysical flow, one of the most prominent features of shocks is heating. Shock heating is responsible for emission in violent phenomena such as supernovae [9, 14], accretion flow [20], and jets [18, 12]. In shocks relativistic effects can be significant. Mathematically, relativistic effects appear in the relativistic Rankine–Hugoniot relations for relativistic hydrodynamics (Taub [7]) and relativistic MHD (Lichnerowicz [4]) as singular perturbations of their nonrelativistic counterparts. This is examplified by the absence of a bound on the ratio on the proper restmass densities (restmass densities in fluid restframe) across shocks, as opposed to the familiar bound $(\gamma+1)/(\gamma-1)$ for the density ratio across shocks (Bazer and Ericson [11]) for polytropic fluids in the nonrelativistic case. This will be illustrated below. In relation to the change of entropy across shocks this indicates that relativistic effects can be dramatic in the emissivity by shocks in astrophysical flows.

In this section, we describe a pseudo-spectral method which enables us to study shock computations in our formulation of MHD (4) with explicit time stepping on a grid $x_1 < x_2 < \cdots < x_N$, $N = 2^M$, with uniform gridspacing $\Delta x = x_{i+1} - x_i = 1/N$. In a specific space–time split (4) may be written in Cartesian coordinates $(x^a) = (t, x^\alpha)$ in flat space–time as

$$\partial_t F^{tA}(t, x^\alpha) + \partial_\alpha F^{\alpha A}(t, x^\alpha) = 0. \tag{11}$$

In all our computations $\xi^a = (\partial_t)^a$. Differentiation of discontinuous fluxes is be removed by taking first the integral of the system with respect to the spatial variable x. We will use this system for each time step. These considerations have led us to set up a numerical scheme, whose derivation consists of three steps. These steps are

Step (a). Write the quantities F^{tA} as a sum of their mean and variational parts

$$F^{tA}(t, x) = F_0^{tA}(t) + F_1^{tA}(t, x), \tag{12}$$

such that $\int F_1^{tA}(t, x)\,dx = 0$. The system of MHD equations thus becomes

$$\partial_t F_1^{tA}(t, x) + \partial_x F_1^{xA}(t, x) = 0, \qquad dF_0^{tA}(t)/dt = 0. \tag{13}$$

Thus, the mean value $F_0^{xA} \equiv \langle F^{xA} \rangle$ of F^{xA} is time invariant. We now proceed with the first half of the equations above.

The quantities F_1^{tA} have zero mean. This allows us to consider the integrated quantities $(F^{tA})^*(t, \cdot)$,

$$(F_1^{tA})^*(t + \Delta t, x) = \int^x F_1^{xA}(t + \Delta t, y)\,dy, \tag{14}$$

of $F_1^{tA}(t, \cdot)$. This integration can be performed efficiently using the fast Fourier transform. Note that the quantities $(F^{tA})^*$ are continuous. These quantities must satisfy

$$\partial_t (F_1^{tA})^*(t, x) + F_1^{tA}(t, x) = 0, \tag{15}$$

where we have used the assumption that F^{xA} vanishes at infinity.

Step (b). Time evolution is performed using the leapfrog method:

$$(F_1^{tA})^*(t + \Delta t, x) = (F_1^{tA})^*(t - \Delta t, x) - 2\Delta t\, F^{xA}(t, x) + O((\Delta t)^3). \tag{16}$$

$F^{tA}(t, x)$ is now obtained from $(F_1^{tA})^*(t, x)$ by differentiation. When using central differencing, the leading error term involves the third derivative of $(F_1^{tA})^*(t, x)$, and, therefore the second derivative of $(F_1^{tA})(t, x)$. Such implicit viscosity can be kept minimal by performing central differencing with Richardson extrapolation:

$$F^{tA}(t + \Delta t, x) = \langle F^{tA} \rangle + \Delta (F_1^{tA})^*(t + \Delta t, x) + O((\Delta x)^2). \tag{17}$$

Here, the Richardson extrapolator, Δ, is given by

$$\Delta f(t, x) = (4\Delta_h f(t, x) - \Delta_{2h} f(t, x))/3 \tag{18}$$

with $\Delta_h f(t, x) = [f(t, x + h) - f(t, x - h)]/2h$.

Step (c). The scheme becomes iterative when using Newton's method to update the family of unknowns U commensurate with the new values $F^{tA}(t + \Delta t, x)$. The Newton's iterations have been carried out with an error criterion of 1.D-07 on the densities F^{tA}. Consequently, the errors in the constraints $u^2 + 1 = 0$ and $c_1 := u^c h_c = 0$ are kept in the order of 1.D-06 in all computations.

In the computations of strong shocks, this scheme yields excessive overshoot. This can be reduced by starting each time step with two times oversampling using an interpolating by

$$f(x_{i+1/2}) \equiv (-f(x_{i-1}) + wf(x_i) + wf(x_{i+1}) - f(x_{i+2}))/(2w - 2). \tag{19}$$

Thus, F^{qA} is defined on a grid with intermediate grid points $x_1 < x_{3/2} < \cdots < x_i < x_{i+1/2} < x_{i+1} < \cdots < x_N < x_{N+1/2}$. Step (a) and Step (b) are carried out on this finer grid, while the last step (c) is applied to F^{tA} on the original, course grid $x_1 < x_2 < \cdots < x_N$ only. This numerical implementation will be used in all our computations.

Note that Step (a) and Step (b) preceded by interpolation (19) result in linear operations. The scheme outlined above, therefore, is of the form

$$(F^{tA})^{m+1} = S_w\{(F^{tA})^{m-1}\} - 2\Delta t\, \delta_w (F^{xA})^m. \tag{20}$$

Here, S_w and δ_w are linear operators on functions on the (coarse) grid $\{x_i\}$, and m denotes the mth time step. The subscript w reflects the parameter dependence in (19). We remark that S_w is a smoothing operator which bears a strong relation to, but is much weaker than, Lanczos smoothing (see, e.g., [23, 2] for Lanczos smoothing). With $w = 9$ interpolation (19) is second order, while in the limit as w goes to infinity, it reduces to a linear interpolation. Finite w thus allows a compromise between accuracy and smoothing.

3.1. *A Test Problem*

We will compute a 1D relativistic Riemann shock-tube problem with purely transverse magnetic field in flat spacetime. The problem setting will be in the context of the coplanar Riemann problem for classical MHD by Brio and Wu [17]. The fluid is assumed to be a monatomic gas with polytropic equation of state,

$$P = Kr^\gamma, \tag{21}$$

relating the pressure, P, and the restmass density, r, with adiabatic constant K and polytropic constant γ. We have taken $\gamma = \frac{3}{2}$, in between its ultrarelativistic limit, $\frac{4}{3}$, and Newtonian limit, $\frac{5}{3}$. Note that this lies below the limit established by Taub: $\gamma \leqslant \frac{5}{3}$ [7]. The adiabatic constant, K, is taken to be $\frac{2}{3}$, uniformly throughout the fluid. We compute the time evolution of fluid on the unit interval, $0 \leqslant x \leqslant 1$, which is initially at rest and possesses an initial jump discontinuity, $[r] = r_{\text{right}} - r_{\text{left}}$, at $x = \frac{1}{2}$. Furthermore, the magnetic flux density, $k = h/r$, where h is the magnetic field strength, also suffers an initial jump at $x = \frac{1}{2}$. In the examples presented below we have taken $k = 1$ for $x < \frac{1}{2}$, and

$k = k_R$ for $x > \frac{1}{2}$. Numerically, the initial conditions at $x = \frac{1}{2}$ are chosen to be the mean of the left and right states.

A detailed error analysis can be given using a comparison solution obtained by the method of characteristics. Recall that a solution to a Riemann shock-tube problem can be described in three parts: increasing with x we find

(1) a simple wave moving into the uniform state at the left. When $K = \frac{2}{3}$, $\gamma = \frac{3}{2}$ and $k = 1$, and using $u^a = (\cosh(\lambda), \sinh(\lambda), 0, 0)$ the state of the fluid can be expressed analytically as [25]

$$\begin{aligned} \lambda + \phi(r) &= J, \\ \phi(r) &= 4 \sinh^{-1}(r^{1/4}), \\ \Lambda &= \tanh(5\lambda/4 - J/4), \end{aligned} \tag{22}$$

where $0 \leqslant \lambda \leqslant \lambda_2$, the value of the Riemann invariant J is given by $\phi(r_{\text{left}})$, and Λ denotes the characteristic velocity;

(2) A uniform state connecting the region with the simple wave solution and the contact discontinuity. Here, the fluid is described simply by $\lambda = \lambda_2$, $r = r_2$, and $h = k_1 r_2 = r_2$ with the continuity condition $\lambda_2 + \phi(r_2) = J$;

(3) A uniform post-shock state in between the contact discontinuity and the shock. Here, the state of the fluid is described by $\lambda = \lambda_2$, $r = r_3$, $P = P_3$, and $h = k_R r_3$ with the jump condition $[F^{aA}(U)]\ v_a(\mu) = 0$ at the shock, where $v^a(\mu) = (\sinh \mu, \cosh \mu, 0)$.

For any initial jump $[r]$ this nonlinear problem in $(\lambda_2, r_3, P_3, \mu)$ can be solved by Newton's method.

A test case is considered with zero initial velocity and longitudinal magnetic field h^x, left state $r_L = 1$, $P_L = \frac{2}{3}$, $(h^y)_L = 1$ and right state $r_R = 0.125$, $P_R = 0.1$, $(h^y)_R = 0.0625$. The initial hydrodynamical data, except for $P_L = \frac{2}{3}$, are those in Sod's shock-tube problem [5], following Roe [21] and Brio and Wu [17]. The solution is shown in Fig. 1 for $n = 256$. The exact solution of this problem is given by the curve with sharp corners in each of the solution panels. Here, the smoothing was done with $w = 12$. The evolution of

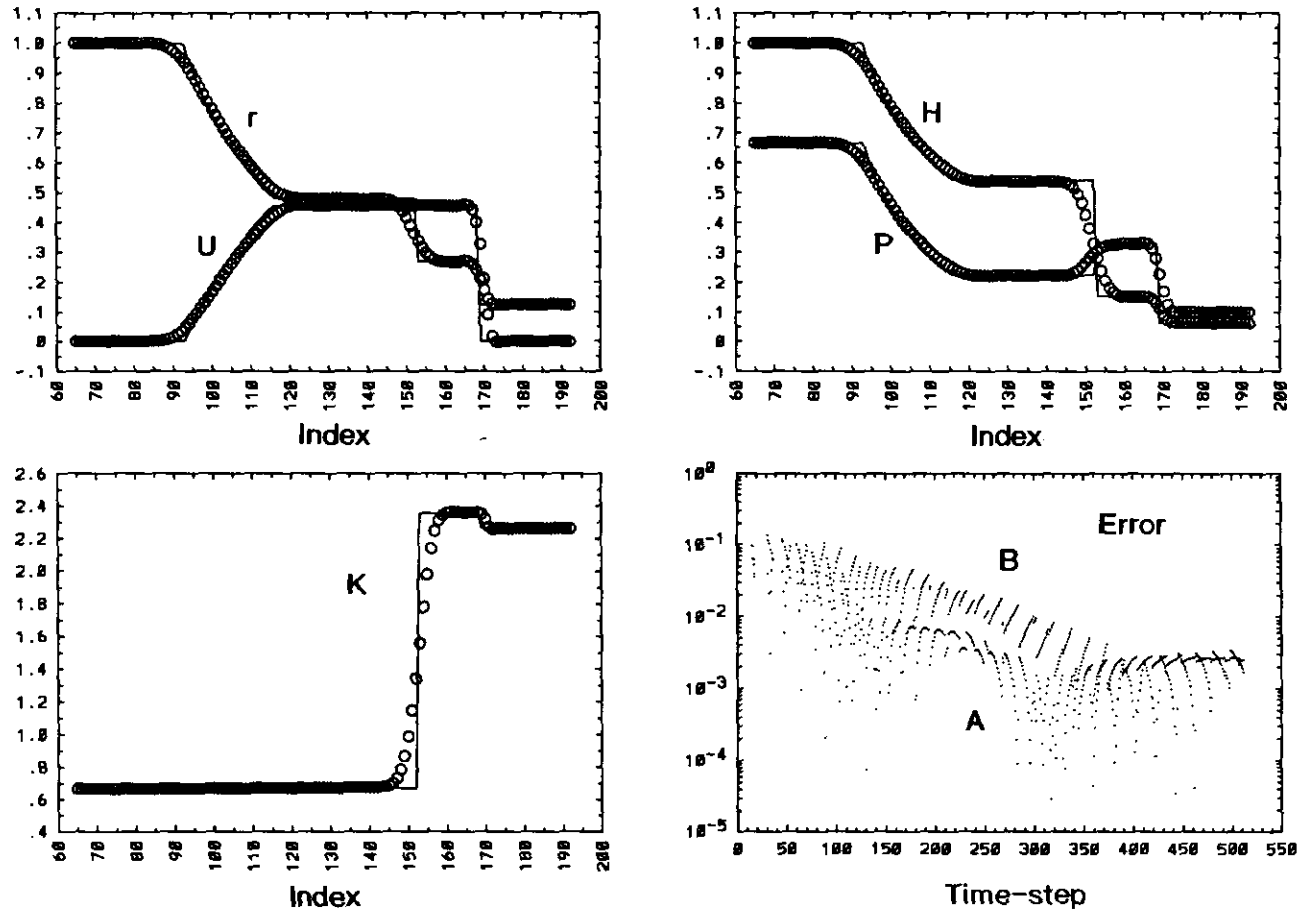

FIG. 1. Numerical solution to shock-tube problem with purely transverse magnetic field in the pseudo-spectral method with $w = 12$. The discretisation is 256 points and 512 time steps with $\Delta t/\Delta x = 0.10$. Convergence of the solution is shown in the lower right panel. Here, averages over the mid one-third of the uniform postshock region (grid points 159 through 164) are compared with the exact solution. The absolute value of the resulting, relative discrepancy is displayed for the velocity (curve A) and restmass density (curve B) at each time-step.

the error with time step m is shown in the lower right panel. Concentrating on the approximation of the shock jump conditions, averages over the mid one-third of the uniform postshock region are compared with the exact solution, and the resulting, relative discrepancy is displayed for the velocity (curve A) and the proper restmass density (curve B). At $m = 516$ the average is over grid points 159–164. Clearly, the results show proper convergence to the exact solution.

We have also studied the effect of smoothing on the quantities in the postshock region. Various values of w, $\eta \equiv \Delta t/\Delta x$ have been considered. Generally, smoothing increases with w and decreases with η. Smoothing by w reaches its maximum at $w = 20$ and minimum at $w = 8$. Table I shows results for various w in the case $n = 512$ at $m = 1032$ time steps with $\eta = 0.10$. Oscillations appear with $w = 8$, a small overshoot remains at the shock when $w = 10$,

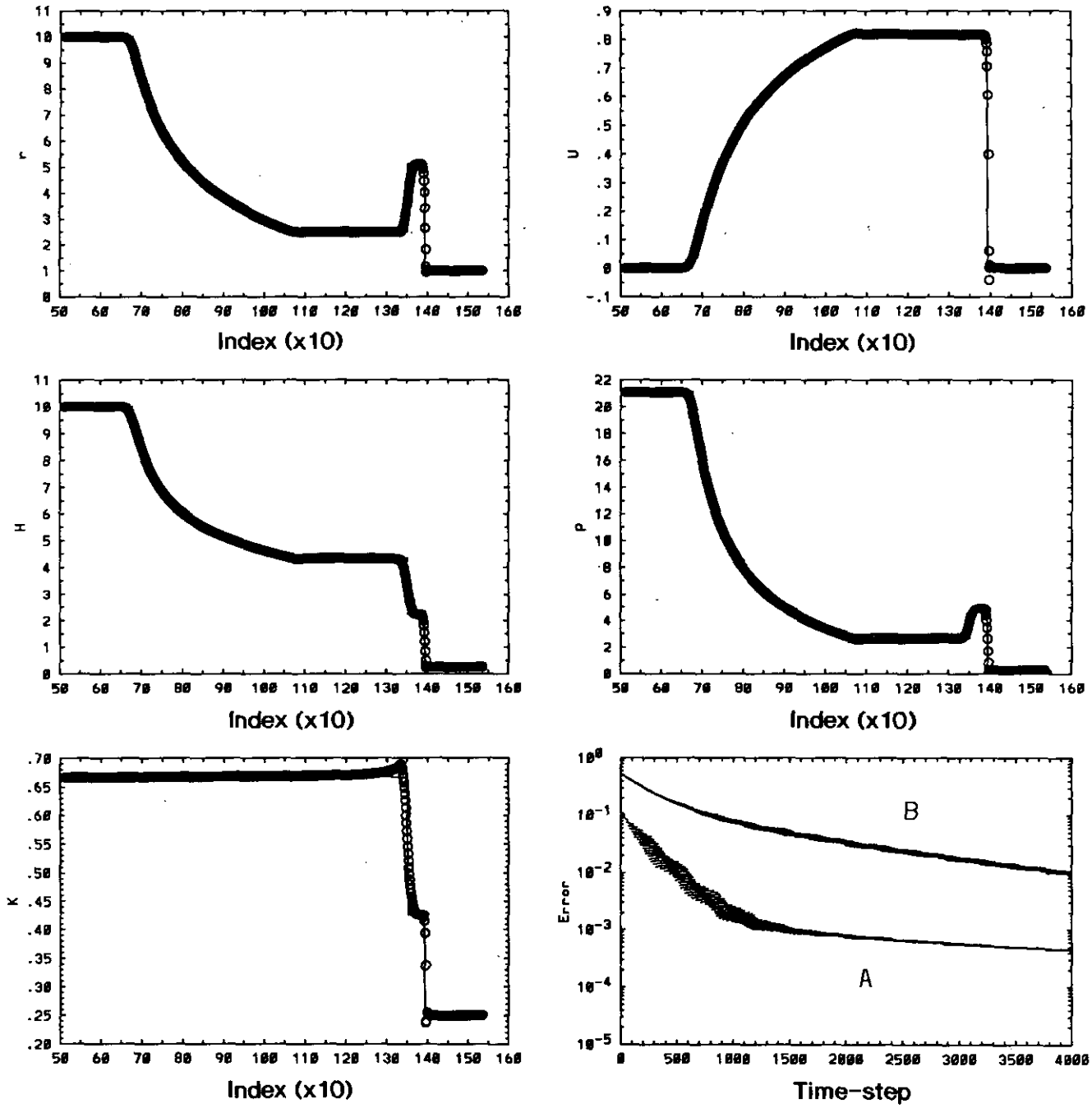

FIG. 2. Numerical solution to shock-tube problem with relativistic shock strength in the pseudo-spectral method with $w = 12$. The discretisation is 2048 points and 4000 time steps with $\Delta t/\Delta x = 0.10$.

TABLE I

Comparison of Numerical Results by Pseudo-Spectral Method for Various Smoothing Values of w with the Exact Solution for the Riemann Problem Shown in Fig. 1 with Discretization $n = 512$

	Pseudo-spectral			
Quantity	$w = 8$	$w = 10$	$w = 12$	Exact
r	0.2695	0.2692	0.2687	0.2693
U	0.4574	0.4562	0.4559	0.4566
H	0.1511	0.1513	0.1511	0.1513
P	0.3299	0.3288	0.3284	0.3292
K	2.3587	2.3534	2.3574	2.3554

Note. The number of time-steps is 1032 with step-size $\Delta t/\Delta x = 0.10$. The numerical values are averages over the mid one-third of the postshock region, grid points 159 through 164.

and no spurious phenomena are present when $w = 12$. Clearly, the results in Table I are remarkably independent of w. Smaller time step sizes $\eta \leqslant 0.05$ give additional smoothing, while $0.10 \leqslant \eta \leqslant 0.15$ yields essentially spurious free results and larger η yield overshoot at the shock.

A strong shock computation is shown in Fig. 2. The initial data are again with zero initial velocity and longitudinal magnetic field h^x, but now with left state $r_L = 10$, $P_L = \frac{2}{3}r^{3/2} \approx 21.08$, $(h^y)_L = 10$ and right state $r_R = 1$, $P_R = 0.25$, $(h^y)_R = 0.25$. Stabilization has been obtained by $w = 12$. Note that the jump in the restmass density across the shock, 5.125 (numerically; 5.140 exact), slightly exceeds the classical bound $(\gamma + 1)/(\gamma - 1) = 5$. Note that although the error is decreasing much slower, there is still convergence.

We conclude that for modest shock strengths suitable choices of the parameters w and η are $10 \leqslant w \leqslant 12$ and $0.10 \leqslant \eta \leqslant 0.15$ with leapfrog time stepping. Strong shock computations can be performed taking w large, $w \geqslant 12$. In all our computations, the approximation of the jump conditions across shocks shows proper convergence.

4. A COPLANAR MHD RIEMANN PROBLEM

We have computed the coplanar Riemann problem for relativistic MHD by application of the pseudo-spectral method to (4). In each computation, initially the velocity u^a and the transverse component h^z are zero throughout and $h_x = h_x^{(0)}\varepsilon$, while $r = 0.125$, $P = 0.1\varepsilon^2$, $h_y = -\varepsilon$ at the right side of the discontinuity at $x = \frac{1}{2}$ and $r = 1$, $P = 1\varepsilon^2$, $h_y = \varepsilon$ at the left side of the discontinuity. We will consider two limiting cases of this Riemann problem. For $\varepsilon \gg 1$ the resulting fluid flow has velocities approaching the speed of light, while for $\varepsilon \ll 1$ the flow has low velocities, pressures, and magnetic field energies (with respect to the restmass energy density, r) and the solutions should approach those of the nonrelativistic equations. Our choice of scaling keeps $\beta = P/h^2 = \text{const.}$ as ε is varied. As a check of our pseudo-spectral method (as opposed to the divergence formulation) we have also used it to solve the classical, nonrelativistic equations solved by Brio and Wu (Eqs. (16)–(22) in [17]). Our low ε and classical results are compared with those of [17] in Table II. For this reason, we have chosen $\gamma = 2$ to facilitate comparison with results from Brio and Wu. In the coplanar Riemann problem, the magnetic field and the velocity are continuous across contact discontinuities whenever the longitudinal magnetic field, h_x, is nonzero. In contrast, $h_x^{(0)} = 0$ does allow these quantities to be discontinuous across contact discontinuities (as in Fig. 1). Thus, $h_x = 0$ with discontinuous magnetic field across a contact discontinuity is a singular limit in MHD. We will illustrate this numerically by consideration of $h_x^{(0)} = \frac{1}{10}$ and $h_x^{(0)} = 0$.

Figures 3–4 show the result for $\varepsilon = 1$, $h_x^{(0)} = \frac{3}{4}$, and $h_x^{(0)} = \frac{1}{2}$, respectively, and Fig. 5 shows the result for $\varepsilon = 0.05$, $h_x^{(0)} = \frac{3}{4}$. Velocities and the transverse magnetic field are depicted twice in Figs. 3–4, once as physical quantities $U = u^x/u^t$, $V = u^y/u^t$, $H^y = u^t h^y - u^y h^t$ in the laboratory frame and once as tensor components $u = u^x$, $v = u^y$, and h^y. The curves of the physical quantities U, V, H^y and the tensor components u^x, u^y, h^y, respectively, coincide to within 0.5% (in the order of the thickness of the lines of the figure) when $\varepsilon = 0.05$. This is the nonrelativistic result of Brio and Wu and a comparison follows below. In each case, the solution consists of a fast rarefaction wave moving to the left, a slow compount wave, a contact discontinuity, and a slow shock and fast rarefaction wave moving to the right (see [17] for the discussion in nonrelativistic MHD). In Fig. 3 the compound wave appears most clearly in the restmass density and the tensor component u^x. Figures 3 and 4 show a pronounced difference between the physical and four-vector components of the tensors. This is due to a jump in the Lorenz factor, Γ, to $\Gamma = 1.428$ in Fig. 3 and to $\Gamma = 1.458$ in Fig. 4. This jump in Γ attenuates the jump in the physical quantities. Furthermore, the rarefaction wave in the compound wave in Fig. 3 is of much smaller amplitude than in Figs. 4 and 5; this rarefaction wave decreases in amplitude with h_x and with velocity. Finally, notice that the heating in the compound wave is negligible compared to the heating in the shock traveling to the right. This follows from the minute jump in K at $x = 0.49$, $x = 0.50$, $x = 0.48$ and the $O(1)$ jump in K at $x = 0.525$, $x = 0.515$, $x = 0.535$ in Figs. 3, 4, and 5, respectively. This suggests that compound waves should they occur in astrophysical flow are not likely to contribute to detectable radiation. We remark that for fluids with $\gamma = \frac{3}{2}$ the numerical results show the same behavior.

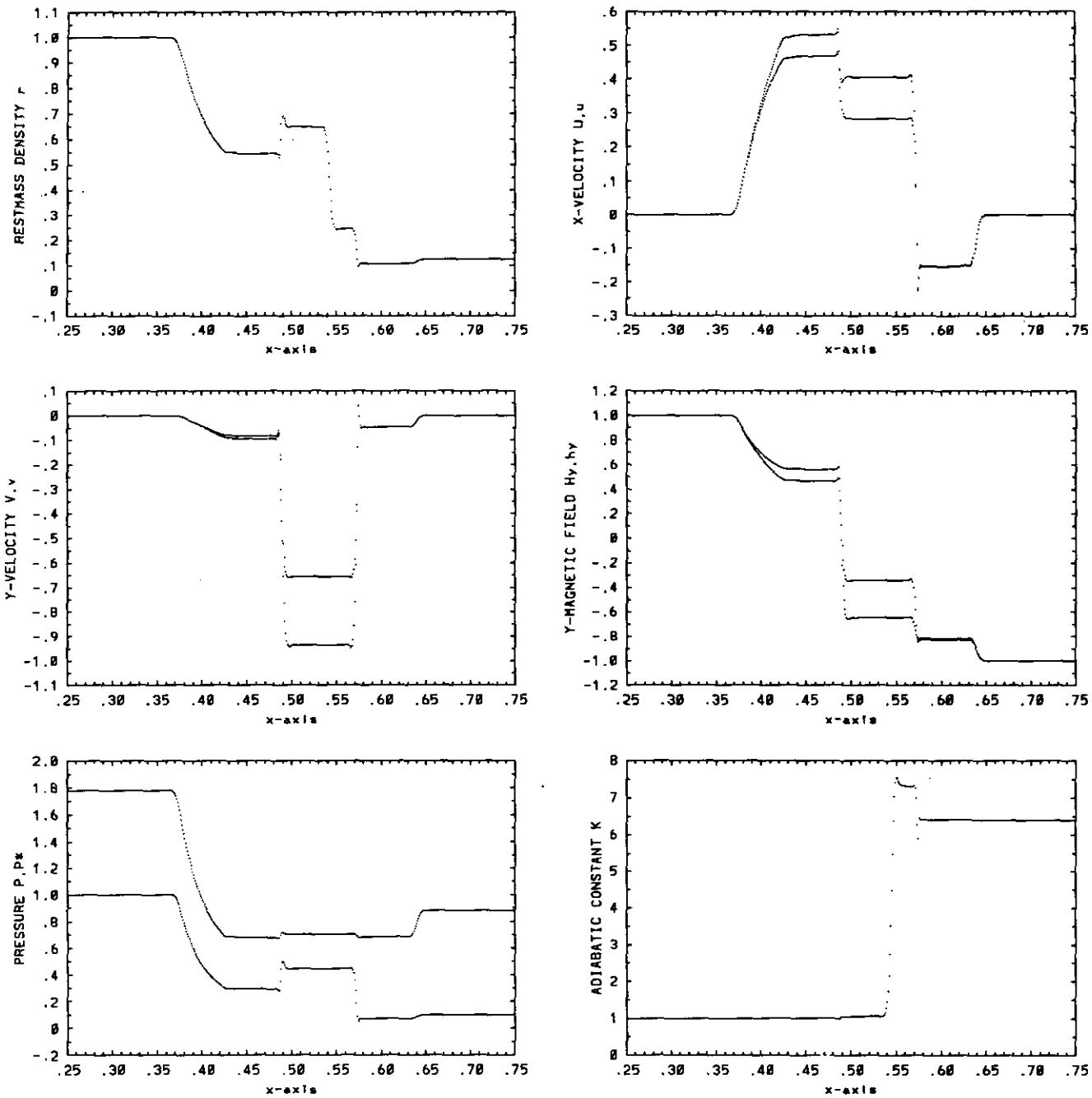

FIG. 3. The pseudo-spectral method on the coplanar Riemann problem for relativistic MHD with $\varepsilon = 1$ and $h_x^{(0)} = \frac{3}{4}$. A small amplitude rarefaction wave is attached to the slow shock traveling to the left, constituting a slow compound wave. The number of time steps is 1000 with 1024 points on the unit interval with $\Delta t/\Delta x = 0.15$. Here, smoothing is with $w = 10$.

4.1. *Limit of Small* $h_x^{(0)}$

The problem in the limit of small $h_x^{(0)}$ is shown in Figs. 6 and 7 for $h_x^{(0)} = \frac{1}{10}$ and $h_x^{(0)} = 0$, respectively. The other parameters are as in Section 4 with $\varepsilon = 1$. Note that as $h_x^{(0)} \to 0$ the transverse velocity has constant magnitude, but is captured in an ever thinner sheet bounded by two slow shocks. When $h_x^{(0)} = 0$, the sheet vanishes, but the spike in P remains. The transverse flux therefore becomes proportional to h_x in this limit, as the jump in h_y approaches finite limits across each of the two shocks. Note that total pressure $P^* = P + h^2/2$ becomes continuous as $h_x^{(0)}$ vanishes. Next consider the limit $h_x^{(0)} = 0$. Since there is a change of sign in h_y across a contact discontinuity approximation of

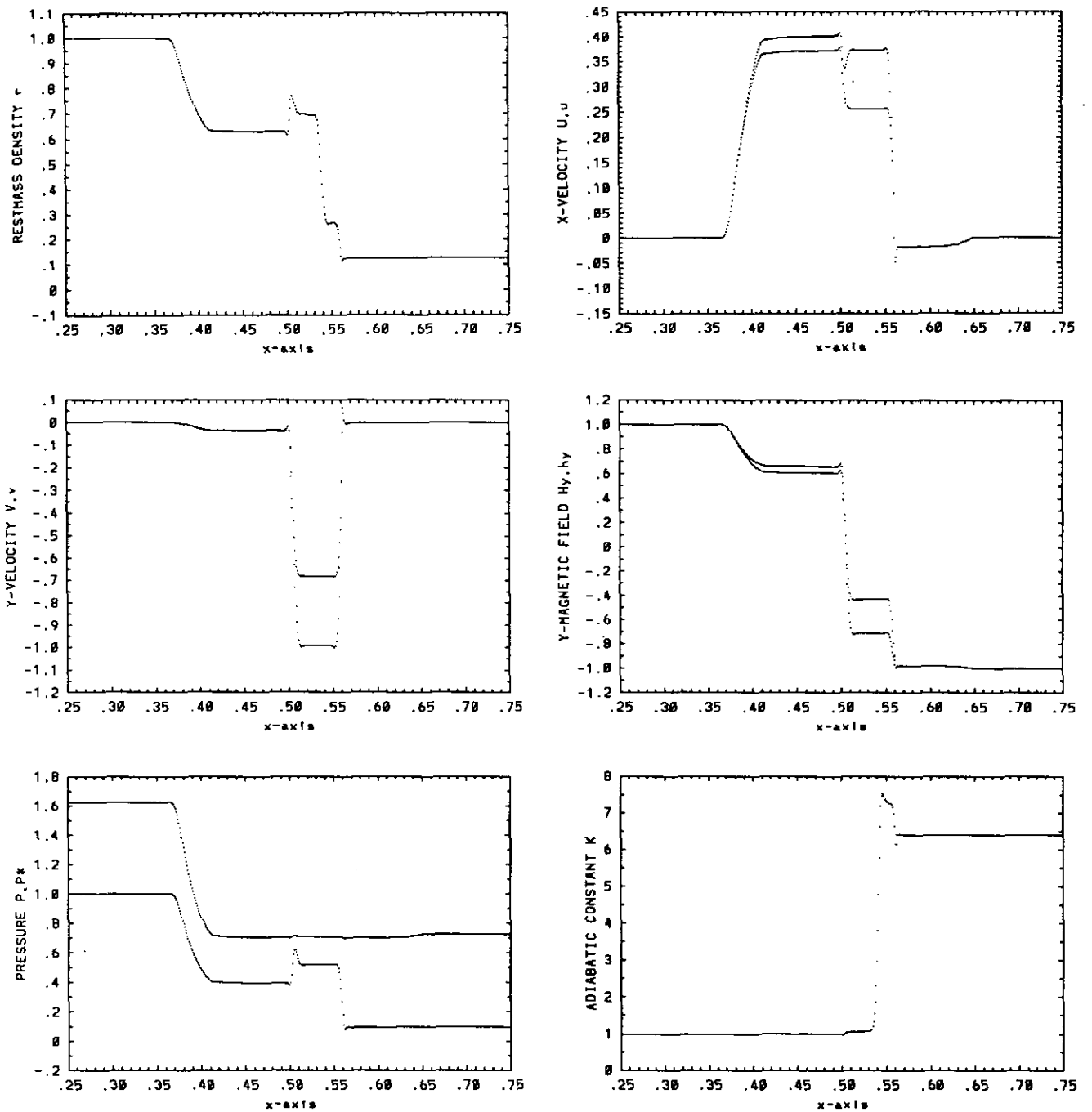

FIG. 4. The pseudo-spectral method on the coplanar Riemann problem for relativistic MHD with $\varepsilon = 1$ and $h_x^{(0)} = \frac{1}{2}$. The numerical parameters are the same as in Fig. 3. The rarefaction wave in the compound wave is now more pronounced than in Fig. 3.

all quantities by smooth functions while keeping the total pressure P^* continuous necessarily requires a large spike in P at the point where h_y changes sign, i.e., goes through zero. Thus, transverse MHD is a singular limit when h_y changes sign across a contact discontinuity. As $h_x^{(0)}$ becomes finite, two waves bifurcate from the contact discontinuity. In this problem these waves are slow shock waves. We remark that when $\gamma = \frac{3}{2}$ the singular nature of this problem is also reflected numerically in a small, erroneous jump in the velocity across the contact discontinuity. The continuity of the total pressure, however, is strictly maintained. We have also considered the small $h_x^{(0)}$ limit on the test problem in Section 1. This yields a bifurcation of the solution near the contact discontinuity into a slow shock and a slow

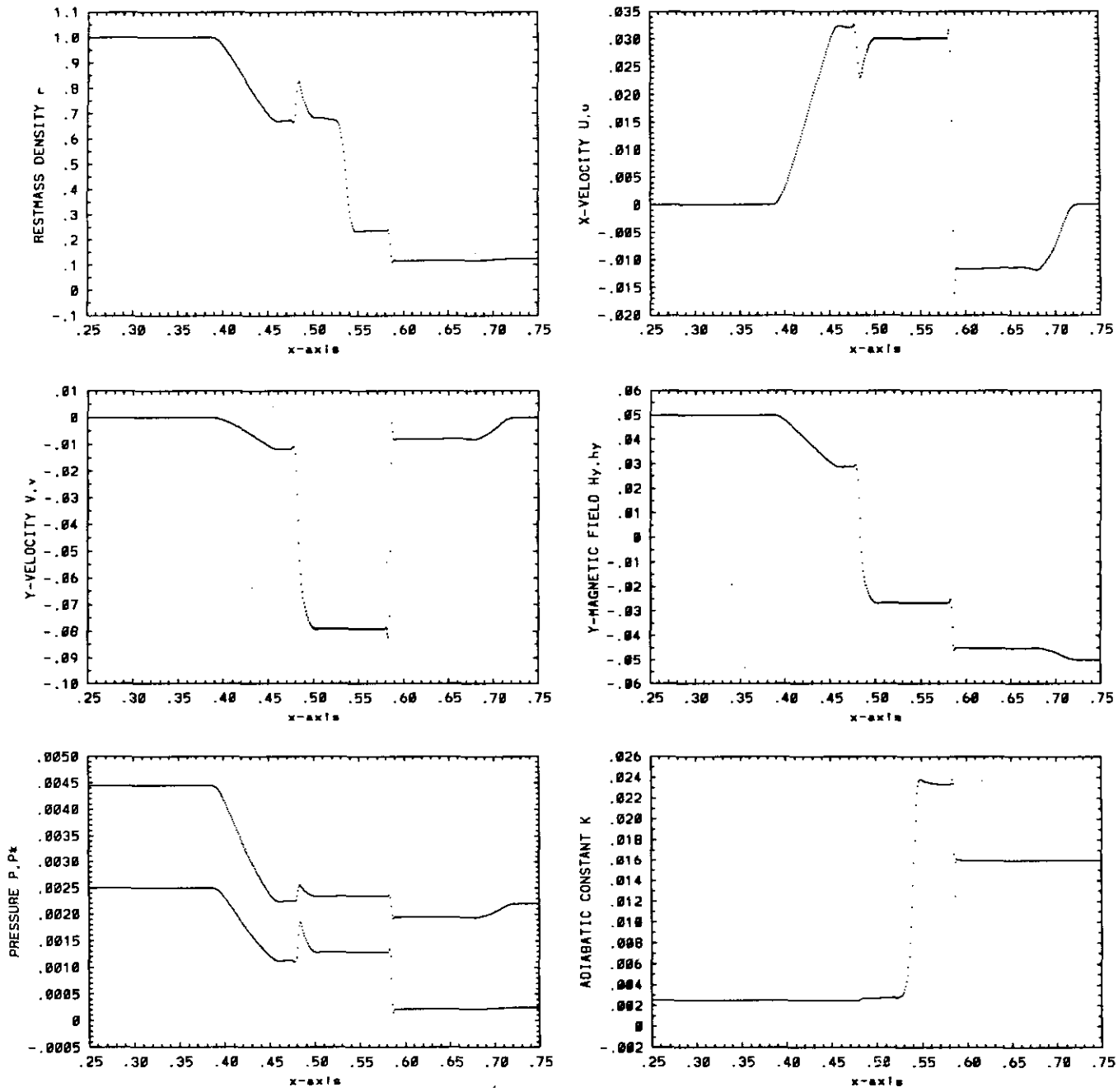

FIG. 5. The pseudo-spectral method on the coplanar Riemann problem for relativistic MHD in the low velocity limit with $\varepsilon = 0.05$, keeping $h_x^{(0)} = \frac{3}{4}$. The number of time steps is 2400 with 1024 points on the unit interval, and the step size is $\Delta t/\Delta x = 0.50$. Smoothing is obtained with $w = 10$.

rarefaction wave. The result is a fast rarefaction wave followed by a slow shock traveling to the left and a fast shock followed by a slow rarefaction wave traveling to the right.

4.2. *Nonrelativistic Limit*

In the limit of nonrelativistic velocities, pressures, and magnetic field energies, our numerical implementation of MHD in divergence form yields nonrelativistic results for the coplanar Riemann problem as shown in Fig. 5. To see this, we will compare these results with those obtained from the equations of nonrelativistic MHD. The difference between the four-vector quantities u, v, h^y and physical quantities U, V, and H^y, respectively, is less than 0.5% when $\varepsilon = 0.05$, as mentioned before, while about 2% when $\varepsilon = 0.10$ (in particular, in U, u and V, v at the right side of the compound wave, where u^t is largest). As $\varepsilon \to 0$, the equa-

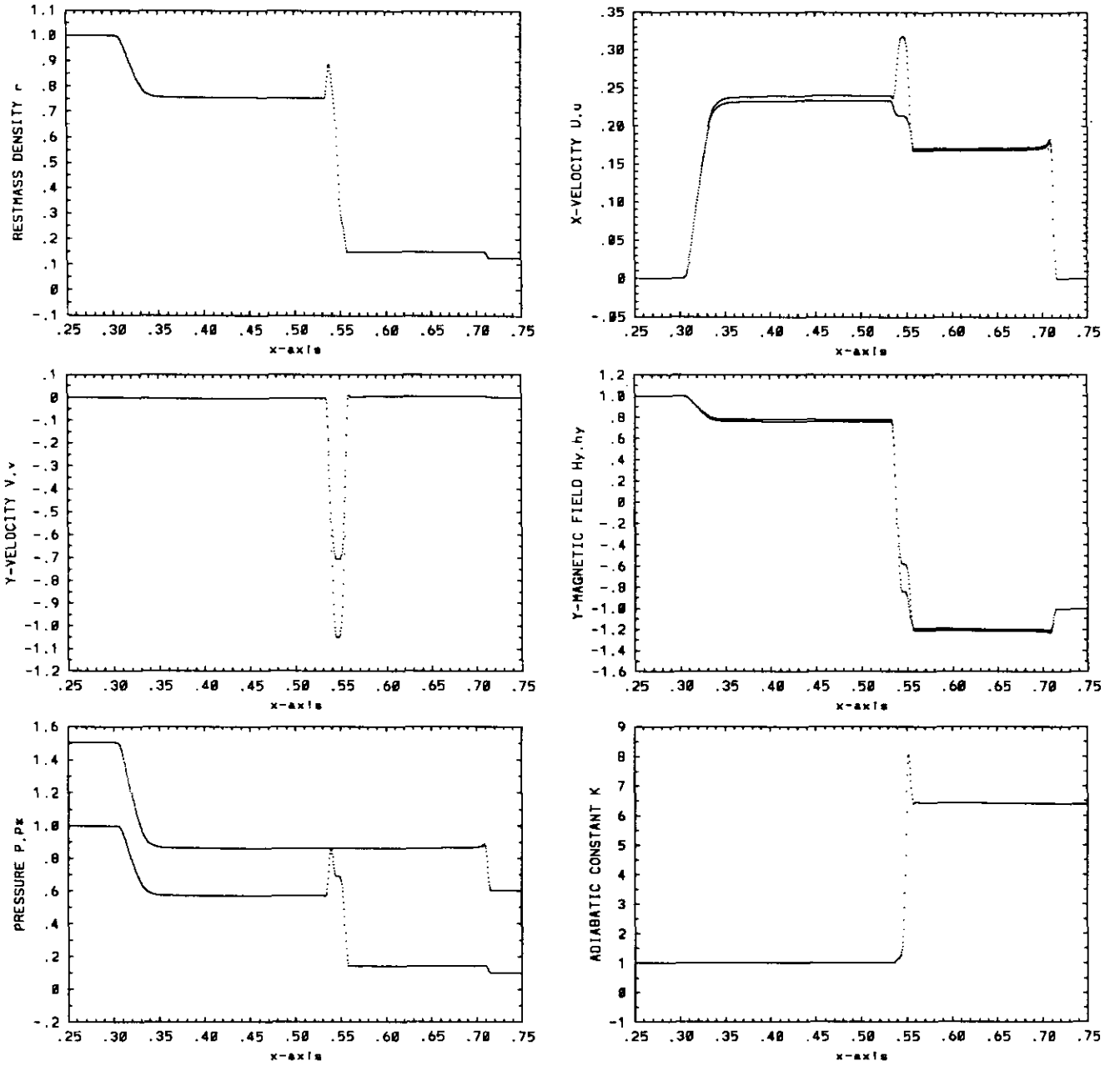

FIG. 6. The low $h_x(0)$ limit showing a bifurcation of two slow shocks from the contact discontinuity. Here, $\varepsilon = 1$ and $h_x^{(0)} = 0.10$. The number of time steps is 3006 with 2048 points on the unit interval, $\Delta t/\Delta x = 0.15$ and $w = 10$.

tions of relativistic MHD reduce to their non-relativistic form [17] which for the coplanar problem amount to

$$\begin{aligned} r_t + (rU)_x &= 0, \\ (rU)_t + (rU^2 + P^*)_x &= 0, \\ (rV)_t + (rUV - H_x H_y)_x &= 0, \\ (H_y)_t + (H_y U - H_x V)_x &= 0, \\ E_t + \{(E + P^*)U - H_x(H_x U + H_y V)\}_x &= 0, \end{aligned} \tag{23}$$

where $P^* = P + (H_x^2 + H_y^2)/2$ and H_x is constant.

The solution to these equations (23) obtained using our pseudo-spectral is shown in Fig. 8. We have estimated the left state before the shock, denoted by subscript L, and the right state at the tail of the rarefaction wave, denoted by subscript R, of the compound wave by taking averages over five points and compared these with data from Brio and Wu [17] and from Stone *et al.* [24]. This is listed in Table II. Note that agreement is typically better than 0.5%, but there is a 1% discrepancy in the proper restmass density on the right side, r_R. We find that this is very sensitive to smoothing (by taking $w \to 20$ and/or smaller time steps

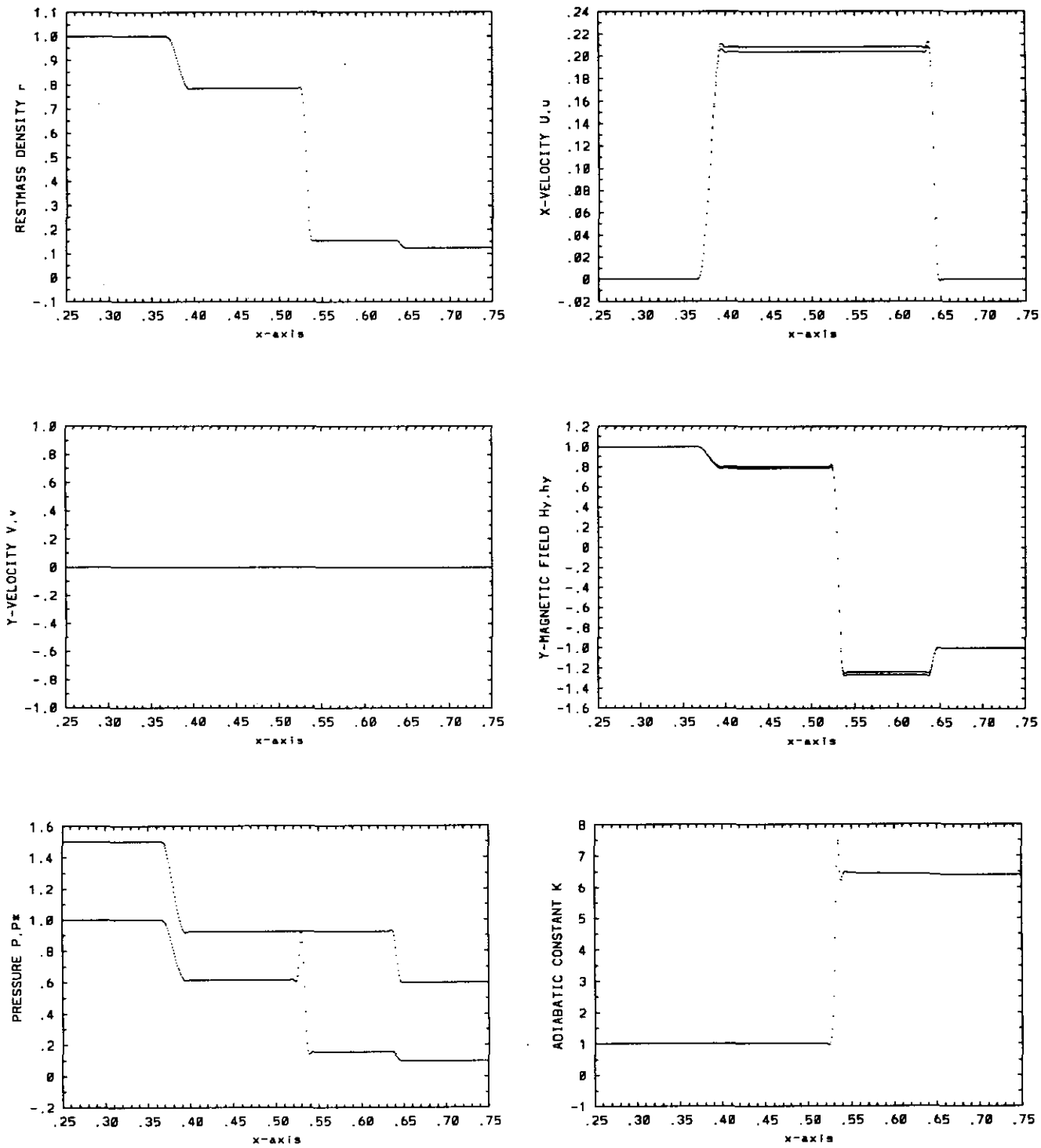

FIG. 7. The singular Riemann problem with $\varepsilon = 1$ and $h_x^{(0)} = 0$. The number of time steps is 1000 with 1024 points on the unit interval, $\Delta t/\Delta x = 0.15$ and $w = 10$.

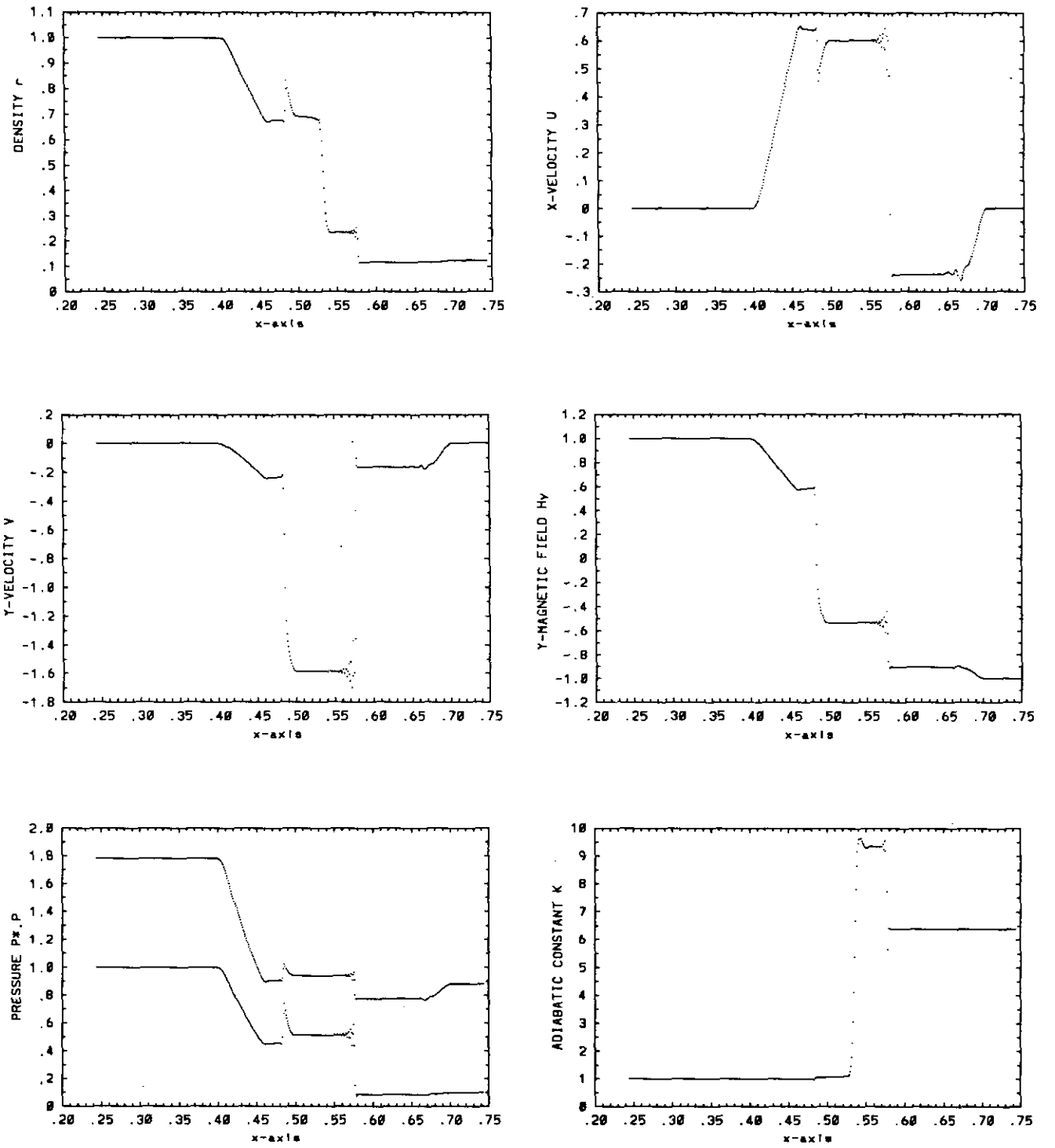

FIG. 8. The pseudo-spectral method on the equations of nonrelativistic MHD. The number of time steps is 360 with 1024 points on the unit interval and $\Delta t/\Delta x = 0.15$. Smoothing is obtained with $w = 12$.

TABLE II

The Low ε Limit of the Relativistic Coplanar Riemann Problem for MHD

Quantity	$\varepsilon = 1$	$\varepsilon = 0.10$	$\varepsilon = 0.05$	$\varepsilon = 0$	Ref. [17]	Ref. [24]
r_L	0.5417	0.6674	0.6722	0.6762	0.6763	0.664
r_R	0.6503	0.6862	0.6844	0.6919	0.6963	0.701
U_L/ε	0.4680	0.6457	0.6427	0.6369	0.6366	0.662
U_R/ε	0.2839	0.5920	0.6002	0.6007	0.5997	0.597
V_L/ε	−8.318E−02	−0.2357	−0.2370	−0.2351	−0.2333	−0.248
V_R/ε	−0.6550	−1.545	−1.576	−1.585	−1.578	−1.58
H_L/ε	0.5619	0.5756	0.5791	0.5835	0.5849	0.576
H_R/ε	−0.3414	−0.5234	−0.5316	−0.5344	−0.5341	−0.536
P_L/ε^2	0.2939	0.4461	0.4528	0.4580	0.4574	0.443
P_R/ε^2	0.4437	0.5115	0.5152	0.5156	0.5133	0.509

Note. Averages of the left and right constant states across the compound wave for various ε and the classical case. Data from Brio and Wu and from Stone *et al.* are listed here for comparison.

$\Delta t/\Delta x \leqslant 0.05$). This may be due to the smoothing at the contact discontinuity, which our method spreads out over about 10 grid points. Interestingly, the appearance of some oscillatory behavior at the shock shows that the nonrelativistic formulation (23) is more difficult to handle with our pseudo-spectral method than the relativistic formulation. This is probably due to a difference in the way conservation of energy is formulated. We have taken $\Delta t/\Delta x = 0.5$ in the low ε relativistic computations and $\Delta t/\Delta x = 0.15$ in the computation on (28). The spurious oscillations in classical MHD disappear when taking smaller time steps ($\Delta t/\Delta x \leqslant 0.05$); however, this introduces smoothing which increases the discrepancy in r_R, as mentioned before.

We conclude form Table II that our numerical implementation of MHD in divergence form shows proper limiting behavior towards nonrelativistic MHD as the velocities, pressures, and magnetic field energies become small.

5. DISCUSSION

The shock computations in this paper show that MHD formulated in divergence form allows stable and accurate numerical simulations. In view of astrophysical applications, emphasis has been given to the computation of the shock heating. With low discretizations the results are particularly accurate for shocks of intermediate strength. The power of the divergence formulation of MHD is brought about by

(c1) convergence of the approximations of the shock jump relations;

(c2) obtaining both relativistic and nonrelativistic results in MHD in divergence form with the same numerical implementation;

(c3) obtaining the above with explicit time-stepping on a uniform grid.

The pseudo-spectral method is a particular form of a smoothing method (see Eq. (20)). The smoothing varies with parameter w and the step size $\Delta t/\Delta x$. The effect of smoothing most clearly appears in shocks and contact discontinuities. In the problems studied in this paper we find that contact discontinuities are resolved best with modest smoothing at the cost of some overshoot at shocks, while essentially spurious free results may be obtained with larger smoothing at the cost of smearing out contact discontinuities over relatively more points. Of course, the particular application at hand determines the optimal amount of smoothing.

We wish to emphasize that the divergence form of MHD in the limit of zero magnetic field yields a divergence form of relativistic hydrodynamics. In view of the results above, this formulation may be competitive with other formulations for relativistic hydrodynamics for the purpose of numerical simulation.

Our computations show that compound waves persist in relativistic MHD. Brio and Wu [17] expressed concern as to whether the compound wave in their computations is physical or a mere artifact of numerical simulation. They do so in view of the slow shock involved being an intermediate shock. We wish to express that in the context of the coplanar Riemann problem, the results of Wu [10], Brio and Wu [17], Stone *et al.* [24] and those contained in this paper lead us to believe that intermediate shocks should be considered natural features in numerical simulations.

ACKNOWLEDGMENTS

With great pleasure the author acknowledges the many fruitful and stimulating discussions with Professor E. Sterl Phinney, and his continued support during this work. The author is very grateful to Professor John F. Hawley for drawing his attention to the work by M. Brio and C. C. Wu, and for his kind permission to include data from Ref. [24].

REFERENCES

1. A. Anile, *Relativistic Fluids and Magneto-Fluids* (Cambridge Univ. Press, Cambridge, UK, 1989).
2. C. Canuto, M. Y. Hussaini, A. Quarteroni, and T. A. Zang, *Spectral Methods in Fluid Mechanics* (Springer-Verlag, Berlin, 1988).
3. A. Lichnerowicz, *Relativistic Hydrodynamics and Magnetodynamics* (Benjamin, New York, 1967).
4. A. Lichnerowicz, Shock waves in relativistic magnetohydrodynamics under general assumptions, *J. Math. Phys.* **17**, 2135 (1976).
5. A. G. Sod, A survey of several finite difference methods for systems of nonlinear hyperbolic conservation laws, *J. Comput. Phys.* **27**, 1 (1978).
6. G. B. Whitham, *Linear and Nonlinear Waves* (Wiley, New York, 1974).
7. A. H. Taub, Relativistic Rankine–Hugoniot equations, *Phys. Rev.* **74**, 328 (1948).

8. E. S. Phinney, *A Theory of Radio Sources*, Ph.D. thesis, Cambridge University, 1983.
9. H. A. Bethe, Supernova mechanisms, *Rev. Mod. Phys.* **62**, 801 (1990).
10. C. C. Wu, On MHD intermediate shocks, *Geophys. Res. Lett.* **14**, 668 (1987).
11. J. Bazer and W. B. Ericson, Hydromagnetic shocks, *Ap. J.* **129**, 758 (1959).
12. K. R. Lind, Numerical jet simulations and parsec-scale jets, in *Parsec-Scale Radio Jets*, edited by J. A. Zensus and T. J. Pearson (Cambridge Univ. Press, New York, 1990).
13. J. M. Marti, J. M. Ibanez, and J. A. Mirallos, Numerical relativistic hydrodynamics: Local characteristic approach, *Phys. Rev. D* **43**, 3794 (1991).
14. L. Herrera and L. A. Nunez, Luminosity profiles and the evolution of shock waves in general-relativistic radiating spheres, *Ap. J.* **364**, 212 (1990).
15. J. F. Hawley, L. L. Smarr, and J. R. Wilson, A numerical study of nonspherical black hole accretion. I. Equations and test problems, *Ap. J.* **277**, 296 (1984).
16. J. F. Hawley, L. L. Smarr, and J. R. Wilson, A numerical study of nonspherical black hole accretion. II. Finite differencing and code calibration, *Ap. J. Suppl.* **55**, 211 (1984).
17. M. Brio and C. C. Wu, An upwind differencing scheme for the equations of ideal magnetohydromagnetics, *J. Comput. Phys.* **75**, 400 (1988).
18. J. O. Burns, M. L. Norman, and D. A. Clarke, Numerical models of extragalactic radio sources, *Science* **253**, 522 (1991).
19. M. R. Dubal, Numerical simulations of special relativistic, magnetic gas-flows, *Comput. Phys.* **64** (2), 221 (1991).
20. P. Meszaros and J. P. Ostriker, Shocks in spherically accreting black holes: a model for classical quasars, *Ap. J.* **273**, L59 (1983).
21. P. L. Roe, Approximate Riemann solvers, parameter vectors, and difference schemes, *J. Comput. Phys.* **43**, 357 (1981).
22. C. R. Evans and J. F. Hawley, Simulation of magnetohydrodynamic flows: a constrained transport method, *Ap. J.* **332**, 659 (1988).
23. R. Peyret and T. D. Taylor, *Computational Methods for Fluid Flow* (Springer-Verlag, New York, 1983).
24. J. M. Stone, J. F. Hawley, R. E. Charles, and M. L. Norman, A test suite for magnetohydrodynamical simulations, *Ap. J.* **388**, 415 (1992).
25. M. H. P. M. Van Putten, Maxwell's equations in divergence form with applications to MHD, *Commun. Math. Phys.* **141**, 63 (1991).
26. Y. Bruhat, Fluides relativiste de conductibilite infinie, *Acta Astronaut.* **6**, 354 (1960).